Theory of severe slowdown in the relaxation of rings and clusters with antiferromagnetic interactions

Ioannis Rousochatzakis,[1,*] Andreas Läuchli,[2] Ferdinando Borsa,[3,4] and Marshall Luban[4]
[1]*Institut de Théorie des Phénomènes Physiques, Ecole Polytechnique Fédérale de Lausanne, CH-1015 Lausanne, Switzerland*
[2]*Max Planck Institut für Physik Komplexer Systeme, D-01187 Dresden, Germany*
[3]*Dipartimento di Fisica "A. Volta," e Unità CNISM, Università di Pavia, I-27100 Pavia, Italy*
[4]*Ames Laboratory and Department of Physics and Astronomy, Iowa State University, Ames, Iowa 50011, USA*
(Received 12 January 2009; published 27 February 2009)

We show that in the severe slowing-down temperature regime the relaxation of antiferromagnetic rings and similar magnetic nanoclusters is governed by the quasicontinuum portion of their quadrupolar fluctuation spectrum and not by the lowest excitation lines. This is at the heart of the intriguing near-universal power-law temperature dependence of the electronic correlation frequency ω_c with an exponent close to 4. The onset of this behavior is defined by an energy scale which is fixed by the lowest spin gap Δ_0. This explains why the experimental curves of ω_c for different cluster sizes and spins nearly coincide when T is rescaled by Δ_0.

DOI: 10.1103/PhysRevB.79.064421 PACS number(s): 75.50.Xx, 76.60.Es

I. INTRODUCTION

A central issue for the control and manipulation of electronic spin degrees of freedom in the field of molecular nanomagnetism[1] and related areas is the understanding and characterization of the various microscopic mechanisms of relaxation and decoherence which stem from the interactions with the underlying degrees of freedom of the host lattice. It is by now well established that in the large majority of magnetic clusters, the relaxation of the magnetization shows a dramatic slowing down which sets in already at relatively high temperatures T and is characterized by a single electronic frequency cutoff ω_c.[1–3] While the majority of freezing mechanisms reported in the literature [e.g., onsite anisotropy in single molecule magnets,[1] anisotropy and critical fluctuations in single chain magnets,[1] and phonon trapping in Ni_{10} (Ref. 4)] has been understood to a large extent on the basis of the nature of the lowest excitations, the case of antiferromagnetic rings (AFMRs) has been exceptional and very intriguing. Indeed, as shown by the nuclear magnetic resonance (NMR) experiments by Baek *et al.*,[5] in the regime where the dramatic slowing-down effect takes place, ω_c follows a near-universal power-law T dependence with an exponent close to 4, a behavior clearly inconsistent with a relaxation scenario based on the lowest excitation lines. It is also striking that the experimental curves of ω_c from various magnetic rings with different sizes and spins $s>1/2$ nearly coincide when T is rescaled by the lowest spin gap Δ_0. On the theoretical side, the first microscopic calculation of ω_c in AFMRs was given by Santini *et al.*,[2] who concluded on this problem that the relevant T regime is too narrow to substantiate any power-law scaling and that instead ω_c is approximately exponential in $1/T$.

Here we present a different microscopic theory which supports the scaling hypothesis of Baek *et al.*[5] and resolves its physical origin in a clear and transparent way. Our central key finding is that in the severe slowing-down T regime, the relaxation is not governed by the lowest excitation lines of the quadrupolar spectral density but by a forest of quasicontinuum excitations at higher energies (cf. Fig. 2). This is at the heart of the power-law temperature dependence of ω_c with an exponent which is close to 4 [cf. Eq. (12)]. The onset of this behavior is defined by an energy scale which is fixed by the lowest spin gap Δ_0, and this explains why curves from different rings fall almost on top of each other when T is rescaled by Δ_0. The present theory is corroborated by a model calculation of the nuclear spin-lattice relaxation rate $1/T_1$ which includes one-phonon, two-phonon, as well as Raman processes and shows excellent agreement with the experimental data for the Cr_8, Fe_6Li, and Fe_6Na clusters.

Our theory is based on the formalism developed in Ref. 3. The advantage of this method is that it is based on an analytical formula which gives ω_c in terms of a frequency overlap between an electronic and a phononic spectral density function [cf. Eqs. (3) or (5) below]. Thus by monitoring the variation in these spectra with T and ω one is able to identify the dominant relaxation channels in each T regime of interest. The central approximation for the derivation of this analytical formula of ω_c is that the spin Hamiltonian $\mathcal{H}_0$ commutes with the total magnetization S_z of the cluster. For the majority of magnetic clusters reported in the literature this approximation is an excellent one for the study of relaxation phenomena at not too low T ($T \gtrsim 1$ K). Indeed, the dominant energy scale in the problem is set by the isotropic Heisenberg exchange and very often by a uniaxial onsite anisotropy. There exist several types of anisotropic interactions which do not conserve S_z, but these are typically very small ($\lesssim 1$ K) and thus play a significant role only at very low T. Thus, although the present work is devoted to the slowing-down mechanism in AFMRs, the method presented here can be applied to the majority of magnetic clusters reported in the literature. In particular, we will argue that the slowing-down mechanism in AFMRs must be common in the general class of antiferromagnetic nanomagnets (which includes, e.g., grids and other clusters) due to their very similar spectral structure (cf. below).

II. METHOD AND MODEL

We consider a magnetic ring with an even number N of spins $s>1/2$ (Ref. 6) described by the Hamiltonian

$$\mathcal{H}_0 = J\sum_i \mathbf{s}_i \cdot \mathbf{s}_{i+1} + g\mu_B B S_z \tag{1}$$

with periodic boundary conditions. The first term describes the antiferromagnetic ($J>0$) exchange between nearest-neighbor spins, the second is the Zeeman energy in a field $\mathbf{B}=B\mathbf{e}_z$, $\mathbf{S}=\Sigma_i \mathbf{s}_i$ is the total spin, $g\simeq 2$, and μ_B is the Bohr magneton. It is known[7–9] that the energy spectrum of $\mathcal{H}_0$ is bounded from below by an excitation band $E_S \simeq \Delta_0 S(S+1)/2$, where $\Delta_0 \simeq 4J/N$ (cf. Ref. 9 for the validity range of this scaling) is the lowest singlet-triplet gap. At higher energies there appears a forest of quasicontinuum excitations which set in progressively above the lowest band. This dense spectral structure above a certain energy scale is very common in finite unfrustrated antiferromagnets[10,11] and, as we show below, affects the relaxational behavior in a very characteristic way.

We are interested in the damping of the equilibrium fluctuations of the total magnetization S_z at not too low T and for $\hbar\omega_e \equiv g\mu_B B \ll J$. This damping is triggered by the (phonon-driven) fluctuating portion of various anisotropies. Here we consider the quadrupolar spin-phonon channel[2,12–14] which we write in the general form

$$\mathcal{V}_{\text{s-ph}} = \sum_{i=1}^{N} \mathbf{Q}(\mathbf{s}_i)\cdot\mathbf{\Phi}(\mathbf{r}_i) \equiv \sum_{i=1}^{N}\sum_{m=-2}^{2} Q_{im}^{\dagger}\Phi_{im}, \tag{2}$$

where $\mathbf{\Phi}(\mathbf{r}_i)$ are functions of the local strains or rotation fields and $Q_m(\mathbf{s}_i)$ are the quadrupolar operators $Q_{\pm 2}(\mathbf{s})=s_{\pm}^2$, $Q_{\pm 1}(\mathbf{s})=(s_{\pm}s_z+s_z s_{\pm})/2$, and $Q_0(\mathbf{s})=s_z^2$.

It has been found, both experimentally[1,5] and numerically,[2] that the damping of S_z is monoexponential (or Markovian) in a large number of nanomagnets. The physical origin of this central feature has been shown[3] to arise from a dynamical decoupling of S_z from the remaining slow degrees of freedom which, in turn, follows from the discreteness of the energy spectrum and the conservation law $[S_z,\mathcal{H}_0]=0$. According to the general expression (27) of Ref. 3, ω_c is given by

$$\omega_c = \frac{\beta}{\chi_0}\sum_{mi,m'i'}\int_0^{\infty} d\omega' J_{F_{im}F_{i'm'}^{\dagger}}(-\omega') J_{\Phi_{im}^{\dagger}\Phi_{i'm'}}(\omega'), \tag{3}$$

where $i\hbar F_{im} \equiv [S_z, Q_{im}] = mQ_{im}$,[15] $\beta = 1/k_B T$, and $\chi_0 \equiv \beta\langle \delta S_z^2\rangle$ is the isothermal susceptibility. Thus ω_c is proportional to the frequency overlap between the absorption ($-\omega'<0$) coefficient $J_{F_{im}F_{i'm'}^{\dagger}}(-\omega')$ and the emission coefficient $J_{\Phi_{im}^{\dagger}\Phi_{i'm'}}(\omega')$ of the host lattice.[16] As we show below, this formulation is very fruitful since it allows one to identify the frequency regime (or the excitations) which gives the dominant contribution to ω_c in the severe slowing-down T regime.

To proceed we shall make the reasonable assumption that the strain fields (e.g., local librations of the ligand groups) are uncorrelated between different magnetic sites, i.e.,

$$J_{\Phi_{im}^{\dagger}\Phi_{i'm'}}(\omega') = J_{\Phi_{im}^{\dagger}\Phi_{im'}}(\omega')\delta_{ii'} \tag{4}$$

(below we drop the site indices since all operators shall refer to a single site). We further note that the SU(2) invariance of $\mathcal{H}_0$ at $B=0$ necessitates that $J_{Q_m Q_{m'}^{\dagger}}(\omega) = J_{Q_1 Q_1^{\dagger}}(\omega)\delta_{mm'}$. Since this remains true at finite B for $k_B T \gtrsim \hbar\omega_e$, we may replace Eq. (3) by

$$\omega_c = \frac{10N}{\hbar^2}\int_0^{\infty} d\omega' \frac{J_s(-\omega')}{\langle \delta S_z^2\rangle} J_{\bar{\Phi}^{\dagger}\bar{\Phi}}(\omega'), \tag{5}$$

where $J_s(\omega) \equiv J_{Q_1 Q_1^{\dagger}}(\omega)$ and

$$J_{\bar{\Phi}^{\dagger}\bar{\Phi}}(\omega) \equiv \sum_m m^2 J_{\Phi_m^{\dagger}\Phi_m}(\omega) \Big/ \sum_m m^2, \tag{6}$$

which defines implicitly an average coupling field $\bar{\Phi}(\mathbf{r},t)$.

For our purposes we use a simple Debye model consisting of three acoustic branches with a common sound velocity c and a Debye cutoff ω_D (cf. below) and keep from the strain tensor[12–14] $\boldsymbol{\epsilon}$ only its isotropic (scalar) portion

$$\eta(\mathbf{r},t) \equiv \nabla\cdot\mathbf{u} = \sqrt{\frac{\hbar}{2Mc}}\sum_{\mathbf{k}\sigma}\sqrt{k}\left(e^{i(\mathbf{k}\cdot\mathbf{r}+\omega_{\mathbf{k}\sigma}t)}a_{\mathbf{k}\sigma}^{\dagger} + \text{H.c.}\right), \tag{7}$$

where $\mathbf{u}(\mathbf{r},t)$ denotes the displacement field, M is the total mass of the crystal, σ runs over the three polarization states, and $\omega_{\mathbf{k}\sigma}=c|\mathbf{k}|$. We may then expand $\bar{\Phi}(\mathbf{r},t)$ as

$$\bar{\Phi}(\mathbf{r},t) \simeq v_1\eta(\mathbf{r},t) + v_2\eta^2(\mathbf{r},t), \tag{8}$$

where v_1 and v_2 define two spin-phonon coupling energy parameters whose importance will become clear below. Since $J_s(\omega)$ is sharply peaked at the Bohr frequencies ω_B of the cluster, i.e., $J_s(\omega)=\Sigma_{\omega_B} J_s'(\omega_B)\delta(\omega-\omega_B)$, we may rewrite Eq. (5) as

$$\frac{\omega_c}{10N} = \sum_{\omega_B>0}\frac{J_s'(-\omega_B)}{\langle \delta S_z^2\rangle}\left[\frac{v_1^2}{\hbar^2}J_{\eta\eta}(\omega_B) + \frac{v_2^2}{\hbar^2}J_{\eta^2\eta^2}(\omega_B)\right]. \tag{9}$$

Using the statistical factor $n(\omega)=(e^{\beta\hbar\omega}-1)^{-1}$ and the mass density ρ_m, we have for $0<\omega<\omega_D$

$$J_{\eta\eta}(\omega) = \frac{3}{2\pi}\frac{\hbar}{\rho_m c^5}n(\omega)\omega^3 \equiv J_{1\text{ph}}(\omega), \tag{10}$$

which is the contribution from direct one-phonon processes, while $J_{\eta^2\eta^2}(\omega)$ is the sum of the two-phonon and Raman contributions given, respectively, by

$$J_{2\text{ph}}(\omega) = A\int_0^{\omega} d\omega'\,\omega'^3 n(\omega')(\omega-\omega')^3 n(\omega-\omega')$$

$$J_R(\omega) = 2A\int_{\omega}^{\omega_D+\omega} d\omega'\,\omega'^3 n(\omega')(\omega'-\omega)^3[n(\omega'-\omega)+1], \tag{11}$$

where $A \equiv \frac{9}{4\pi^3}\frac{\hbar^2}{\rho_m^2 c^{10}}$. These processes are represented schematically in Fig. 1.

Equations (9)–(11) are the starting point of our calculations for ω_c. The quadrupolar spectral density $J_s(\omega)$ is obtained by a full thermodynamic calculation using exact diagonalizations.

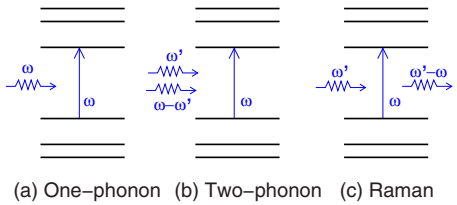

FIG. 1. (Color online) Schematic representation of the three lowest-order processes which contribute to ω_c for any given absorption frequency ω of the nanomagnet. (a) The one-phonon absorption process is proportional to the average phonon energy density $\omega\rho(\omega)n(\omega)$, where $\rho(\omega)$ is the phonon density of states and $n(\omega)=[\exp(\beta\hbar\omega)-1]^{-1}$ is the Bose-Einstein distribution function. (b) The two-phonon absorption process is proportional to the integral $\int d\omega'\omega'\rho(\omega')n(\omega')(\omega-\omega')\rho(\omega-\omega')n(\omega-\omega')$. (c) The inelastic-scattering Raman process is proportional to the integral $\int d\omega'\omega'\rho(\omega')n(\omega')(\omega'-\omega)\rho(\omega'-\omega)[n(\omega'-\omega)+1]$.

III. SLOWING-DOWN EFFECT AND NEAR-UNIVERSAL POWER-LAW SCALING

Figure 2 shows $J_s(-\omega)$, $J_{1\mathrm{ph}}(\omega)$, $J_{2\mathrm{ph}}(\omega)$, and $J_R(\omega)$ for Cr_8 at $\hbar\omega_e=0.066\Delta_0$ and for (a) $k_BT=0.19\Delta_0$ and (b) $2.22\Delta_0$. The values of the parameters used here are the ones that fit

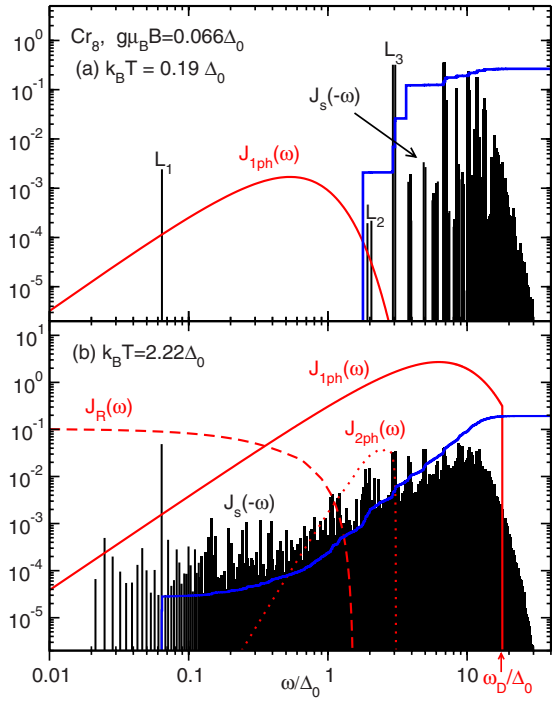

FIG. 2. (Color online) The origin of the dramatic slowing-down effect in AFMRs demonstrated here for the Cr_8 cluster at (a) $k_BT=0.19\Delta_0$ and (b) $2.22\Delta_0$, with $\hbar\omega_e=0.066\Delta_0$ and $\hbar\omega_D=10J$. The correlation frequency ω_c is proportional [cf. Eqs. (3) or (5)] to the overlap between the quadrupolar spin density $J_s(-\omega)$ (series of δ peaks shown here with a logarithmic mesh in ω) and the phononic density $J_{\bar{\Phi}^\dagger\bar{\Phi}}(\omega)$ which includes one-phonon (solid red), two-phonon (dotted red), and Raman (dashed red) processes. We also show (thick solid blue line) the integrated density $\int_0^\omega d\omega' J_s(-\omega')$. The lowest three groups of excitation lines at low T are denoted by L_1, L_2, and L_3 (cf. text).

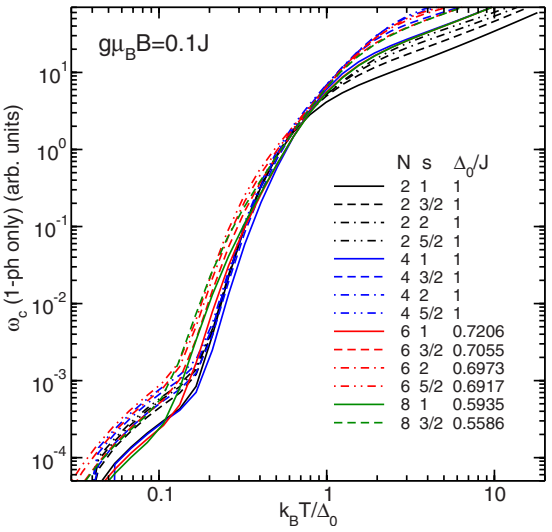

FIG. 3. (Color online) Near-universal behavior of ω_c vs k_BT/Δ_0 for rings with different N and s. The dramatic slowing down (by 3 and 4 decades) takes place in the regime $0.2\Delta_0\lesssim k_BT\lesssim 2\Delta_0$, where ω_c follows Eq. (12). The limits of this distinctive T regime can be understood by looking at Fig. 2. It begins when the one-phonon spectral peak starts overlapping the quasicontinuum portion of the quadrupolar density and terminates when it has sampled its entire bandwidth. At $k_BT\gtrsim 2\Delta_0$, $\omega_c\propto T$ (Raman processes or high-frequency phonons alter this behavior), while at very low T, $\omega_c\sim\omega_e^3/(e^{\beta\hbar\omega_e}-1)$ (cf. text).

the $1/T_1$ data (cf. Table I). Apart from identifying a number of excitation lines such as L_1 (transitions within the lowest triplet), L_2 (transitions from the lowest triplet to the lowest quintet), and L_3 (transitions from the lowest singlet to the lowest quintet),[17] we find a number of general features which originate in the overall spectral structure of AFMRs described above. We first emphasize the increasingly gapped structure at low ω and T, and the fact that $J_s(-\omega)$ has essentially no weight below the line L_2. This structure is altered very quickly by thermal excitations since the latter increase the number of available resonant channels and thus give rise to a dense fluctuation spectrum at higher T. Importantly, $J_s(-\omega)$ remains appreciable over an overall bandwidth of $\hbar\omega_{\max}\sim 10-20\Delta_0$. Given now the behavior of the phononic density (cf. Fig. 2) the relaxation process can be understood as follows. At $k_BT\lesssim\hbar\omega_e\ll\Delta_0$ the system is essentially opaque to the available (thermally excited) phonons since there is no appreciable overlap between $J_s(-\omega)$ and $J_{1\mathrm{ph}}(\omega)$. Only the Zeeman line L_1 contributes, giving $\omega_c\sim\omega_e^3/(e^{\beta\hbar\omega_e}-1)$. However, as soon as the one-phonon spectral peak reaches the quasicontinuum regime (above the line L_2), significant number of spin-phonon resonant channels are quickly thermally activated. In fact, Fig. 2(b) shows that $J_{1\mathrm{ph}}(\omega)$ samples almost the entire electronic spectral weight up to $\omega_{\max}$ already at $k_BT\sim 2\Delta_0$. This marks the existence of a special regime $0.2\Delta_0\lesssim k_BT\lesssim 2\Delta_0$, where a dramatic change in ω_c by 3 and 4 decades (cf. Fig. 3) takes place. We emphasize here that the relaxation process in this T regime is driven by the quasicontinuum portion of the quadrupolar spectrum and is minimally affected by the lowest excitation lines. This shows that ω_c is not a nearly exponential function

in $1/T$ in this regime. In fact, we may go one step further and inquire into the observed power-law scaling by employing a steepest-descent expansion in Eq. (5) which relies on two central ingredients: (i) the dominant contribution to the overlap comes from the regime around the one-phonon peak $\hbar\omega_p(T) \simeq 2.82 k_B T$ (note that Fig. 2 is in logarithmic scale) and (ii) the quasicontinuum character of $J_s(-\omega)$ in the respective T and ω regimes. To leading order

$$\omega_c \propto T^4 f(T), \tag{12}$$

where $f(T) \equiv J_s[-\omega_p(T), T]/\chi_0 T$ and the strong T^4 prefactor emerges from the functional form of $J_{1\mathrm{ph}}(\omega, T)$ alone. The function $f(T)$ varies with N and s but shows always a much weaker (sublinear) T dependence. This can be seen by our calculations shown in Fig. 4 (cf. text below) which are in excellent agreement with experimental data. Hence, the $T^{3.5\pm0.5}$ scaling law reported in Ref. 5 is largely due to the above T^4 leading prefactor. It is thus essentially a characteristic fingerprint of one-phonon acoustic processes and of the quasicontinuum nature of the electronic quadrupolar spectrum at high energies.

All of the above features are demonstrated in Fig. 3 which shows the one-phonon contribution to ω_c for various N and s. Indeed, one identifies a distinctive regime $0.2\Delta_0 \lesssim k_B T \lesssim 2\Delta_0$, where ω_c shows a dramatic drop by 3 and 4 decades. Figure 3 explains yet another of the central findings of Baek *et al.*,[5] namely, that all curves fall almost on top of each other when plotted against $k_B T/\Delta_0$. This is clearly due to the overall similar spectral structure of AFMRs and, in particular, due to the fact that the forest of quasicontinuum excitations sets in at an energy scale fixed by $\Delta_0 \simeq 4J/N$ (and not by J).

We should add here that the details of the low-energy spectrum such as the character of the lowest L band or the spin-wave E band[8] do not play any special role compared to other excitations. The quasicontinuum portion of the spectrum contains excitations from and toward both the L and E bands but it is the global dense aspect of the spectrum that matters.

IV. COMPARISON TO NUCLEAR SPIN-LATTICE RELAXATION RATE DATA

Let us now describe our calculations for $1/T_1$ and compare to the experimental data for Fe_6Li, Fe_6Na, and Cr_8. We begin with the expression[2,5,18]

$$1/T_1 = \mathcal{A}_{zz} J_{s_{0z}s_{0z}}(\omega_L) = \frac{\mathcal{A}_{zz}}{N^2} J_{S_z S_z}(\omega_L) \tag{13}$$

where $\mathbf{s}_0$ is the ionic spin with the shortest distance r_0 from the nuclear spin and $\mathcal{A}_{zz} = \hbar^2 \gamma_e^2 \gamma_n^2 / r_0^6$ is the corresponding hyperfine amplitude.[19] Using[3] $J_{S_z S_z}(\omega_L) = 2\langle \delta S_z^2 \rangle \frac{\omega_c}{\omega_c^2 + \omega_L^2}$ and $\chi_{\mathrm{mol}} = N_A g^2 \mu_B^2 \beta \langle \delta S_z^2 \rangle$ (where N_A is Avogadro's number), we get

$$R \equiv \frac{1}{T_1 \chi_{\mathrm{mol}} T} = 4585.3 \frac{\gamma_n^2}{N^2 r_0^6} \frac{\omega_c}{\omega_c^2 + \omega_L^2}, \tag{14}$$

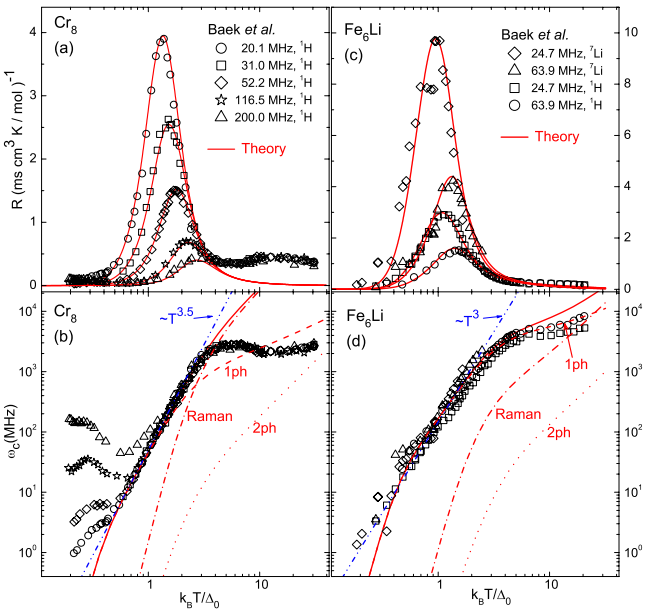

FIG. 4. (Color online) Comparison between theory (solid red lines) and experimental data (symbols) for R [cf. Eq. (14)] and ω_c for Cr_8 (left) and Fe_6Li (right). The one-phonon (dashed), two-phonon (dotted), and Raman (dashed dotted) contributions to ω_c are also shown, along with the respective power-law scalings (dashed-double dot, blue lines) for $0.2\Delta_0 \lesssim k_B T \lesssim 2\Delta_0$.

where $1/T_1$ is given in milliseconds, γ_n is given in MHz/T, $\chi_{\mathrm{mol}} T$ is given in cm^3 K/mol, r_0 is given in Å, and $\omega_{c,L}$ is given in MHz. According to Eq. (14), the fit of r_0 is controlled by the magnitude of $1/T_1$, while the values of v_1 and v_2 of Eq. (9) can be found by adjusting the position and the width of the $1/T_1$ peak. We should note however that v_2 affects ω_c only at the high-T side of the peak where high-energy phonons start to play a role and thus its estimate is generally less accurate.

Figure 4 shows our optimal fits to the data of R and ω_c for Cr_8 and Fe_6Li, along with the separate contributions of direct two-phonon and Raman processes. Similar fits (not shown here) are obtained for Fe_6Na. The corresponding estimates for r_0, v_1, and v_2 are given in Table I and are of the correct order of magnitude. As to the value of the Debye cutoff, we find that our fits remain very good for $\hbar\omega_D \sim 10J$,[20] which is consistent with the reported estimates of the Debye temperature Θ_D [cf. Table I]. The agreement at intermediate T, where the enhancement of $1/T_1$ takes place, is remarkably good. In particular, we find that the relaxation is dominated by one-phonon processes up to $k_B T \sim 2\Delta_0$ for Cr_8 ($\Delta_0/k_B \simeq 9.607$ K) and up to $\sim 6\Delta_0$ for Fe_6Li ($\Delta_0/k_B \simeq 14.526$ K). On the other hand, the power-law scaling (dashed-double dot blue lines) is valid up to $k_B T \sim 2\Delta_0$ for both clusters. We also find that our model does not account for the behavior at very high T. This can be either due to another contribution to $1/T_1$ [e.g., electronic T_2 processes[18,21,22] not included in Eq. (14)] or due to the actual details of the high-energy phonon modes which should play a role at high T. Finally, the discrepancy at very low T in Cr_8 arises from an additional peak in $1/T_1$ which is currently not understood.

TABLE I. Known data (Refs. 23 and 24) (first three columns) and fitting parameters for Fe_6Li, Fe_6Na, and Cr_8. Here $\tilde{c} \equiv \frac{c[\mathrm{cm/s}]}{2\times 10^5}$.

Cluster	ρ_m (g/cm^3)	Θ_D (K)	J (K)	$v_1/\tilde{c}^{5/2}$ (K)	$v_2/\tilde{c}^5$ (K)	r_0 (Å)
Fe_6Li	1.45	217.8	21	0.498	2.861	4.59
Fe_6Na	1.42	209.8	28	0.200	1.277	4.16
Cr_8	1.08	154 ± 10	17.2	1.124	14.376	4.10

V. CONCLUSIONS

We have presented a microscopic theory which identifies the mechanism responsible for the dramatic slowing-down effect observed in antiferromagnetic wheels. Our central key result is that in this class of nanomagnets the relaxation is driven by the quasicontinuum portion of the quadrupolar spectrum and not by the low-lying excitations. This is at the heart of the intriguing power-law T dependence of the electronic correlation frequency ω_c with an exponent close to 4. The onset of this scaling is fixed by the lowest spin gap $\Delta_0 \simeq 4J/N$ (and not by J), and this explains why the experimental curves of ω_c for different cluster sizes and spins nearly coincide when T is rescaled by Δ_0. Since the spectral structure of AFMRs is very common in finite-size antiferromagnets most of the above qualitative features must carry over to other antiferromagnetic clusters as well. Hence we believe that the present slowing-down mechanism of AFMRs is common in the more general class of antiferromagnetic clusters. More generally, the present theory can be applied to the majority of clusters reported in the literature for $T \gtrsim 1$ K. It can also be extended to clusters with $s=1/2$ by using an appropriate relaxation channel.[6] It is thus our hope that it will be valuable for further investigations on the understanding and characterization of relaxation mechanisms in magnetic nanoclusters.

ACKNOWLEDGMENTS

We thank F. Mila and M. Belesi for fruitful discussions. The work at EPFL was supported by the Swiss National Fund. Work at the Ames Laboratory was supported by the Basic Energy Sciences, Department of Energy under Contract No. DE-AC02-07CH11358.

*ioannis.rousochatzakis@epfl.ch

[1] D. Gatteschi, R. Sessoli, and J. Villain, *Molecular Nanomagnets* (Oxford University Press, Oxford, 2006) (and references therein).
[2] P. Santini, S. Carretta, E. Liviotti, G. Amoretti, P. Carretta, M. Filibian, A. Lascialfari, and E. Micotti, Phys. Rev. Lett. **94**, 077203 (2005).
[3] I. Rousochatzakis, Phys. Rev. B **76**, 214431 (2007).
[4] S. Carretta, P. Santini, G. Amoretti, M. Affronte, A. Candini, A. Ghirri, I. S. Tidmarsh, R. H. Laye, R. Shaw, and E. J. L. McInnes, Phys. Rev. Lett. **97**, 207201 (2006).
[5] S. H. Baek, M. Luban, A. Lascialfari, E. Micotti, Y. Furukawa, F. Borsa, J. van Slageren, and A. Cornia, Phys. Rev. B **70**, 134434 (2004).
[6] Magnetic clusters with $s=1/2$ must be treated separately since they do not have a quadrupole moment and thus a different relaxation channel (e.g., dipolar channel or fluctuating Dzyaloshinskii-Moriya interactions) must be invoked.
[7] J. Schnack and M. Luban, Phys. Rev. B **63**, 014418 (2000).
[8] O. Waldmann, Phys. Rev. B **65**, 024424 (2001).
[9] L. Engelhardt and M. Luban, Phys. Rev. B **73**, 054430 (2006).
[10] C. Lhuillier, arXiv:cond-mat/0502464 (unpublished).
[11] For frustrated clusters see, e.g., I. Rousochatzakis, A. M. Läuchli, and F. Mila, Phys. Rev. B **77**, 094420 (2008).
[12] J. Villain, F. Hartman-Boutron, R. Sessoli, and A. Rettori, Europhys. Lett. **27**, 159 (1994); F. Hartmann-Boutron, P. Politi, and J. Villain, Int. J. Mod. Phys. B **10**, 2577 (1996).
[13] M. N. Leuenberger and D. Loss, Phys. Rev. B **61**, 1286 (2000).
[14] E. M. Chudnovsky, D. A. Garanin, and R. Schilling, Phys. Rev. B **72**, 094426 (2005).
[15] As expected, only the $m \neq 0$ components of $\mathbf{Q}$ can drive the relaxation of S_z.
[16] Here, the spectral density for any pair of operators A and B is defined as $J_{AB}(\omega) = \int_{-\infty}^{\infty} dt e^{i\omega t} \langle A(0)B(t) \rangle$.
[17] Note that there is no absorption line at $\Delta_0 \pm \hbar\omega_e$ since transitions from the ground state to the lowest triplet are forbidden by symmetry for our quadrupolar spin-phonon coupling.
[18] I. Rousochatzakis, Ph.D. thesis, Iowa State University, 2005.
[19] For ^{7}Li NMR in Fe_6Li, one must multiply Eq. (13) with an extra factor of $N=6$ since the nuclear spin resides at the center of the ring and thus all ions contribute equally to the nuclear relaxation.
[20] This is an approximate lower bound of ω_D since, as can be understood from Fig. 2, larger values do not alter ω_c quantitatively at intermediate T.
[21] L. Spanu and A. Parola, Phys. Rev. B **72**, 212402 (2005).
[22] B. Pilawa, R. Boffinger, I. Keilhauer, R. Leppin, I. Odenwald, W. Wendl, C. Berthier, and M. Horvatić, Phys. Rev. B **71**, 184419 (2005).
[23] G. L. Abbati *et al.*, Inorg. Chem. **36**, 6443 (1997); A. Caneschi *et al.*, Angew. Chem., Int. Ed. Engl. **34**, 467 (1995); J. van Slageren *et al.*, Chem.-Eur. J. **8**, 277 (2002).
[24] M. Affronte, J. C. Lasjaunias, and A. Cornia, Eur. Phys. J. B **15**, 633 (2000); M. Affronte, T. Guidi, R. Caciuffo, S. Carretta, G. Amoretti, J. Hinderer, I. Sheikin, A. G. M. Jansen, A. A. Smith, R. E. P. Winpenny, J. van Slageren, and D. Gatteschi, Phys. Rev. B **68**, 104403 (2003).